An Approximate Model and Empirical Energy Function for Solute Interactions with a Water-Phosphatidylcholine Interface

Charles R. Sanders II and James P. Schwonek
Department of Physiology and Biophysics, Case Western Reserve University School of Medicine, Cleveland, Ohio 44106 USA

ABSTRACT An empirical model of a liquid crystalline (L_α phase) phosphatidylcholine (PC) bilayer interface is presented along with a function which calculates the position-dependent energy of associated solutes. The model approximates the interface as a gradual two-step transition, the first step being from an aqueous phase to a phase of reduced polarity, but which maintains a high enough concentration of water and/or polar head group moieties to satisfy the hydrogen bond-forming potential of the solute. The second transition is from the hydrogen bonding/low polarity region to an effectively anhydrous hydrocarbon phase. The "interfacial energies" of solutes within this variable medium are calculated based upon atomic positions and atomic parameters describing general polarity and hydrogen bond donor/acceptor propensities. This function was tested for its ability to reproduce experimental water-solvent partitioning energies and water-bilayer partitioning data. In both cases, the experimental data was reproduced fairly well. Energy minimizations carried out on β-hexyl glucopyranoside led to identification of a global minimum for the interface-associated glycolipid which exhibited glycosidic torsion angles in agreement with prior results (Hare, B. J., K. P. Howard, and J. H. Prestegard. 1993. *Biophys. J.* 64:392–398). Molecular dynamics simulations carried out upon this same molecule within the simulated interface led to results which were consistent with a number of experimentally based conclusions from previous work, but failed to quantitatively reproduce an available NMR quadrupolar/dipolar coupling data set (Sanders, C. R., and J. H. Prestegard. 1991. *J. Am. Chem. Soc.* 113:1987–1996). The proposed model and functions are readily incorporated into computational energy modeling algorithms and may prove useful in future studies of membrane-associated molecules.

INTRODUCTION

Bilayers composed of a limited number of purified phospholipids are routinely used as models for natural membranes in a variety of biophysical studies. Because of recent innovations in areas such as solid state nuclear magnetic resonance (Smith and Peersen, 1992) and attenuated total reflection infrared spectroscopy (Braiman and Rothschild, 1988), many such biophysical studies are now focussing upon the orientations, conformations, and dynamics of biomolecules associated with bilayers. However, data from these studies are often insufficient to elucidate total three-dimensional and dynamic structure, dictating a need for complementary computational methods to fill gaps left by the experimental data. Because of the theoretical and computational formidability of modeling bilayer lipid-solute interactions *ab initio*, approximate methods may often be the approach of necessity.

The most commonly studied model membrane system is that of liquid crystalline (L_α phase) phosphatidylcholine (PC). Some investigators have computationally modeled bilayers composed of this phospholipid using explicit molecules (De Loof et al., 1991), while others have chosen the opposite extreme: generalizing the water-lipid interface as an instantaneous change from a bulk aqueous phase to a bulk hydrocarbon phase (Nyholm et al., 1989). Between these extremes lie the Marcelja functions which have been used in molecular dynamics simulations of phosphatidylcholine (Marcelja, 1974; De Loof et al., 1991; Pastor et al., 1991). However, the Marcelja functions are not generally applicable but were designed to model the dynamics of *long-chained* amphiphiles.

A more general set of approaches (Edholm and Jahnig, 1988; Brasseur et al., 1982; Ram et al., 1992) approximate the lipid-water interface to be a gradual transition from a high dielectric medium to a low dielectric medium. Experimental support for suitability of this approximation is summarized in the Discussion section. Edholm and Jahnig (1988) proposed a hydrophobic potential energy function for molecules interacting with this variable medium based upon the position of atoms (or entire amino acid side chains) and atomic/group hydrophobic parameters. Brasseur et al. (1982) also parameterized chemical groups according to their water to apolar phase transfer energies, but also modulated *intramolecular* electrostatic energies according to position within the variable dielectric medium using a standard dielectric constant-dependent electrostatic energy function. Prestegard and co-workers (Ram et al., 1992) proposed a function which calculates solute-medium interaction energies based upon balancing the unfavorable energy associated with solute cavity formation with a favorable electrostatic solute-medium interaction term.

Even if the approximation of the interface as a continuous gradient is satisfactory, there remain difficulties with the three approaches described above. In the empirical approaches based on free energies of transfer, parameterization has previously been made by approximating the apolar region of the bilayer interface in terms of a *single* solvent. In fact, no one single solvent can simultaneously approximate both the effectively anhydrous center of the bilayer and the

Received for publication 11 February 1993 and in final form 17 June 1993.
Address reprint requests to Charles R. Sanders II.
© 1993 by the Biophysical Society
0006-3495/93/09/1207/12 $2.00

nonpolar, but somewhat water-saturated region of the interface near the ester linkages of the acyl chains. The quantitative approach of Ram et al. (1992) is highly dependent upon the choice of partial atomic charges and upon the way in which dipole cavity sizes are estimated. Furthermore, while the free energy associated with cavity formation in a bulk aqueous phase as opposed to a bulk apolar phase is relatively easy to model, less is known about how to model such energies in *mixed* phases such as water-organic solvent mixtures or within the polar to nonpolar transition region of a PC bilayer.

In this study, reliance is made upon the general conceptual treatment of the interface employed in the studies summarized above (7–9). However, the water-PC interface is now approximated to be a gradual *two-step* transition between three phases. The first transition is from a bulk aqueous phase to a nonpolar phase which retains the ability to satisfy the hydrogen bonding potential of a solute due to the presence of significant quantities of water and/or polar lipid moieties. The second transition is from this fairly nonpolar (but hydrated) phase to an effectively anhydrous hydrocarbon phase. This model draws heavily upon the neutron diffraction results of Wiener and White (1992) which map the positional distributions of water and lipid moieties along the bilayer normal of an L_α-PC interface. While there are alternate ways of qualitatively describing this medium, the two-step transition model has been chosen because of the availability of results from previous studies dedicated to uncovering the relationships between hydrogen bonding, solvent polarity, and solute partitioning: most notably, a good deal of effort has gone into accounting for the difference in partitioning of solutes between water and octanol (nonpolar, but water-saturated and capable of hydrogen bonding) and between water and effectively anhydrous hydrocarbons (Kamlet et al., 1988; El Tayer et al., 1991). Based upon the proposed two-step model and the results of these previous studies, a method for calculating interface-solute interaction energies is presented and tested in this paper.

It should be noted that Milik and Skolnick (1993) recently presented an interfacial energy function which also defines a bilayer in terms of gradual transitions between water, "interface," and hydrocarbon phases. However, their method is peptide-specific and defines the partitioning energy in terms of summed contributions from five different effects, an approach which also borrows heavily upon the work of the White lab (i.e., Jacobs and White (1989)), but in a manner dissimilar from that presented herein.

METHODS AND THEORY

Model for the membrane interface

The z axis is defined as the direction of the bilayer normal:

For $z \leq 0$:

$$\epsilon = 76.5 * \exp\{-[(z - z_0)/A]^2\} + 2.0. \quad (1a)$$

For $z > 0$:

$$\epsilon = 80.5 - (76.5 * \exp[-((-z - z_0)/A)^2] + 2.0). \quad (1b)$$

z_0 was set to 3.85 so that the midpoint of a transition from a high ($\epsilon = 78.5$) to low ($\epsilon = 2$) dielectric medium occurs at $z = 0$. The z dependency of ϵ defined by these equations is illustrated in Fig. 1 *A*.

Both the exponential shape of the transition function and the width of the dielectric transition (A) were chosen based on the neutron scattering results of Wiener and White (1992), taking the experimental z-dependent variation in interfacial water concentration to be proportional to the local dielectric constant. Based on these results, A was set to 4.63 Å. As described below, this total transition is defined to span two energetically distinct domains: $\epsilon = 78.5$ to 10 and $\epsilon = 10$ to 2. The crucial $\epsilon = 10$ point occurs at $z = -3.1$ according to Eq. 1.

Calculation of interfacial energies

In the range of $\epsilon = 78.5$ to 10, the atomic interfacial energies are described based upon an "empirical atomic polarity" (Po)

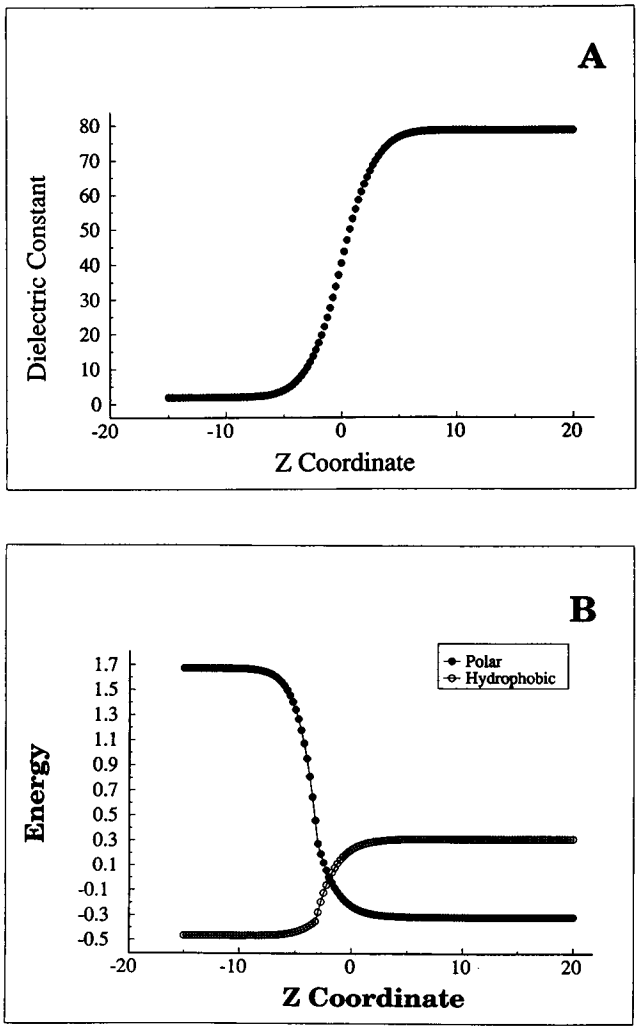

FIGURE 1 (*A*) Dependence of local dielectric constant (ϵ_{curr}) upon position along the bilayer normal (z, in angstroms) defined by Eq. 1. (*B*) Interfacial energies (kcal/mol) of virtual hydrophobic ($P_o = 0.5$, $N_C = 1$) and polar ($P_o = -0.5$, $\beta = -0.5$) atoms predicted by Eqs. 2 and 3. The $\epsilon_{curr} = 10$ point which defines the boundary dividing governance of the energy by the two equations occurs at $z = -3.1$.

TABLE 1 Parameters used in interfacial energy calculations

Atom type*‡	P_o§¶	β	α
$\underline{C}H_3R,CH_4$	-0.6771	0	0
R–$\underline{C}H_3$‖	0.869	0	0
$\underline{C}H_2R_2$	-0.4873	0	0
R–$\underline{C}H_2$–R‖	0.580	0	0
$\underline{C}HR_3$	-0.3633	0	0
$R_3\underline{C}H$‖	0.181	0	0
$\underline{C}R_4$	-0.1366	0	0
$\underline{C}H_3X$	-1.0824	0	0
$\underline{C}H_2RX$	-0.8370	0	0
$\underline{C}H_2X_2$	-0.6015	0	0
$\underline{C}HR_2X$	-0.5210	0	0
$\underline{C}HRX_2$	-0.4042	0	0
$\underline{C}HX_3$	0.3651	0	0
$\underline{C}R_3X$	-0.5399	0	0
$\underline{C}R_2X_2$	0.4011	0	0
$\underline{C}RX_3$	0.2263	0	0
$\underline{C}X_4$	0.8282	0	0
$=\underline{C}H_2$	-0.1053	0	0
$=\underline{C}HR$	-0.0681	0	0
$=\underline{C}R_2$	-0.2287	0	0
$=\underline{C}HX$	-0.3665	0	0
$=\underline{C}RX$	-0.9188	0	0
$=\underline{C}X_2$	-0.0082	0	0
Ar $\underline{C}H$	0.0068	-0.017	0
Ar $\underline{C}R$	0.1600	-0.017	0
Ar $\underline{C}X$	-0.1033	-0.017	0
Ar R–$\underline{C}H$–X	0.0598	-0.017	0
Ar R–$\underline{C}R$–X	0.1290	-0.017	0
Ar R–$\underline{C}X$–X	0.1652	-0.017	0
Ar X–$\underline{C}H$–X	0.2975	-0.017	0
Ar Xz–$\underline{C}R$–X	0.9421	-0.017	0
Ar X–$\underline{C}X$–X	0.2074	-0.017	0
R–($\underline{C}$=X)–R	0.0956**	0	0
Ar–($\underline{C}$=X)–R	-0.1116	0	0
R–($\underline{C}$=X)–X	0.0709	0	0
$\underline{H}$–C^0_{sp3}	0.4418	0	0
$\underline{H}$–C^1_{sp3}	0.3343	0	0
$\underline{H}$–C^0_{sp2}	0.3343	0	0
$\underline{H}$–C^2_{sp3}	0.3161	0	0
$\underline{H}$–C^1_{sp2}	0.3161	0	0
$\underline{H}$–C^3_{sp3}	-0.1488	0	0
$\underline{H}$–OR (1°)	-0.620**	0	-0.32
$\underline{H}$–OR (2°)	-0.620**	0	-0.31
$\underline{H}$NHR	-0.3260	0	-0.025
$\underline{H}$–NR_2	-0.3260	0	-0.025
$\underline{H}$–S	-0.3260	0	-0.025
(C=O)N–$\underline{H}$	-0.3260	0	-0.25
(C=O)O–$\underline{H}$	-0.3260	0	-0.55
Ar–O–$\underline{H}$	-0.3260	0	-0.61
Ar–N$\underline{H}$	-0.3260	0	-0.13
$\underline{H}$–αC	0.2099	0	0
$\underline{H}$–C^0_{sp3}–CX	0.3695	0	0
$\underline{H}$–C^0_{sp3}–CX_2	0.2697	0	0
$\underline{H}$–C^0_{sp3}–CX_3	0.3647	0	0
$R^{1°}$–$\underline{O}$–H	-0.0804	-0.45	0
$R^{2°}$–$\underline{O}$–H	-0.0804	-0.51	0
X–C_{sp3}–C–$\underline{OH}$	-0.568	-0.48	-0.32
(C=$\underline{O}$)–$\underline{O}$–H	0.4860	-0.15	0
Ar–$\underline{O}$–H	0.4860	-0.23	0
R–(C=$\underline{O}$)–R	-0.3514	-0.48	0
R–(C=$\underline{O}$)–O	-0.3514	-0.30	0
R–(C=$\underline{O}$)–N	-0.3514	-0.45	0
R–$\underline{O}$–R	0.1720	-0.47	0
R–(C=O)–$\underline{O}$–R	0.2712	-0.15	0
R–$\underline{N}H_2$	0.1187	-0.68	0
R_2–$\underline{N}$H	0.2805	-0.70	0
R_3–$\underline{N}$	0.3954	-0.68	0
Ar–$\underline{N}H_2$	0.3132	-0.50	0
Ar–$\underline{N}$HR	0.4238	-0.50	0
Ar–$\underline{N}R_2$	0.8678	-0.50	0
R(C=O)–$\underline{N}$	-0.0528	-0.33	0
Ar $\underline{N}$	-0.1106	-0.42	0

as follows:

$$G_{int} = (0.646 - 11.46/\epsilon_{curr}) \cdot 2.3 \cdot RT \cdot P_o \qquad (2)$$

where ϵ_{curr} is determined by the atom's current z coordinate (Eq. 1). The factor of $(0.646 - 11.46/\epsilon_{curr})$ varies from +0.5 to −0.5 as ϵ_{curr} varies from 78.5 to 10. The form of this factor was chosen based upon its similarity to the ϵ-dependent scaling of electrostatic interactions of the Born equation (Bergethon and Simons, 1990). P_o were primarily taken from the work of Viswanadhan et al. (1989) where atom types were assigned P_o according to their empirical contribution to the water-octanol log K_p of nearly 900 compounds (K_p is the partitioning coefficient). Octanol has a dielectric constant of 10.3. The energies predicted by Eq. 2 for a virtual hydrophobic atom and a virtual polar (and hydrogen bond accepting) atom are represented in Fig. 1 *B* in the $z = -3.1$ to +20 region of the plot.

One problem with the P_o taken from Viswanadhan et al. (1989) is that they seriously underestimate log K_p for aliphatic hydrocarbons. This stems from the fact that pure aliphatic hydrocarbons (with no polar groups) and molecules with long alkyl chains represent only a small fraction of the hundreds of molecules from which aliphatic carbon and hydrogen P_o were derived. As a result, the original parameters for the atoms of these groups are skewed in favor of higher polarities. To correct for this effect, all available octanol-H_2O log K_p data for strictly aliphatic hydrocarbons (see Table 2) were fit as a function of the number of CH_3, CH_2, CH, and C in the solute. This led to the estimates for the methyl, methylene, and methine *group* P_o given in Table 1 and provided an excellent reproduction of the experimentally observed partitioning energies (see aliphatic series in Table 2). Similar considerations also led to modification of the original parameters for alcohol O and H as well as ketone carbons.

When a solute atom is positioned along z such that ϵ_{curr} falls between 10 and its minimum value of 2, the interfacial energy is calculated as:

$$G_{int} = -2.3RTP_0/2 + \frac{\epsilon_{curr} - 10}{8} \cdot 2.3RT(1.96\beta + 3.4\alpha + 0.091N_C + 0.31N_{CX} + 0.045N_{AR}) \qquad (3)$$

where α and β are empirical parameters describing (respectively) the hydrogen bond donating and accepting capabilities of the atom in question. N_C, N_{CX}, and N_{AR} have values

* Atoms for which parameters apply are boldfaced and underlined. In cases where more than one atom is boldfaced and underlined, the parameters apply to the *entire group*.

‡X, heteroatom (O, N, P, S); Ar, aromatic. For C^n_{sp2}, n is the oxidation number (defined as the number of bonds made by the carbon to a heteroatom (double bonds count twice)).

§For definition of parameters, see Theory section.

¶P_o, the more negative, the more polar.

‖The aliphatic group parameters apply to carbons separated by at least three bonds from the nearest heteroatom (C–C–C–X) or at least two bonds from the nearest carbonyl, aromatic, or alkenyl carbon.

**Modified from the values originally reported by Viswanadhan et al. (1989).

TABLE 2 Observed and predicted water-solvent solute partitioning energies (kcal/mol) at 25°C

Compound	ΔG_{oct}*‡ (predicted)	ΔG_{oct} (observed)	$\Delta G_{HC} - \Delta G_{oct}$§ (observed)	$\Delta G_{HC} - \Delta G_{oct}$¶ (predicted)
Methanol	−1.05	−1.05	−2.75	−2.25
Ethanol	−0.60	−0.42	−2.44	−2.13
1-Propanol	0.343	0.34	−2.41	−2.00
1-Butanol	1.13	1.20	−2.25	−1.88
1-Pentanol	1.92	2.12	−2.66	−1.76
1-Hexanol	2.71	2.76	−2.15	−1.63
1-Heptanol	3.49	3.28	−1.91	−1.51
1-Octanol	4.19	4.28	NA‖	NE‖
Dodecanol	7.40	6.98	NA	NE
Isobutanol	0.96	1.03	−2.36	−1.88
2-Propanol	−0.03	0.07	−2.67	−2.12
tert-Butanol	0.07	1.03	−2.36	−1.99
Benzene	2.78	2.10	0.20	0.09
Toluene	3.42	3.71	0.22	0.22
Ethylbenzene	4.25	4.28	0.38	0.34
Benzyl alcohol	1.36	1.50	−2.34	−2.15
Phenol	2.40	1.99	−3.11	−3.34
4-Methylphenol	3.03	2.64	−2.90	−3.23
2-Naphthol	3.76	3.86	−3.45	−3.28
Pyridine	2.26	0.88	−1.30	−1.04
Aniline	1.72	1.22	−1.18	−1.83
Benzamide	0.95	0.87	−3.97	−4.29
Acetanilide	1.22	1.58	−3.89	−3.01
Acetic acid	−0.23	−0.23	−3.71	−3.62
Butyric acid	1.71	1.07	−2.38	−3.37
Hexanoic acid	3.29	2.61	−2.28	−3.12
Decanoic acid	6.44	5.56	NA	NE
Ethane	2.36	2.46	0.69	0.25
Propane	3.15	3.21	0.83	0.37
Cyclopropane	2.37	2.34	NA	NE
Butane	3.94	3.93	0.99	0.50
Isobutane	3.79	3.75	NA	NE
Pentane	4.73	4.61	1.20	0.62
Neopentane	4.32	4.23	NA	NE
Cyclopentane	3.84	4.08	NA	NE
Cyclohexane	4.74	4.68	0.96	0.75
Hexane	5.52	NA	NA	0.75
2,2-DMB	5.10	5.19	NA	NE
2,3-DMB	5.21	5.24	NA	NE
Acetone	−0.48	−0.33	−0.91	−1.03
Butanone	0.68	0.39	−0.73	−0.91
2-Pentanone	1.33	1.24	−0.66	−0.78
2-Hexanone	2.11	1.86	−0.68	−0.66
Methyl acetate	−0.185	0.25	−0.60	−0.65
Ethyl acetate	0.90	0.99	−0.60	−0.53
Propylacetate	1.78	1.69	−0.47	−0.40
Acetamide	−1.40	−1.42	−4.97	−4.27
Methyl acetamide	−1.07	−1.43	NA	NE
DMA	−0.73	−1.05	NA	NE
Ethylamine	−0.37	−0.37	−2.04	−1.49
Propylamine	0.80	0.65	−2.01	−1.37
Butylamine	1.36	1.32	−2.16	−1.25
Diethylamine	0.65	0.77	−1.61	−0.88
Dipropylamine	2.52	2.27	−0.19	−0.63
Trimethylamine	0.21	0.37	−1.02	−0.54
Ethylene glycol	−1.94	−2.61	−3.87	−4.51
Glycerol	−2.92	−2.67	−5.17	−6.87
1,2-Propanediol	−1.38	−1.84	−3.86	−4.51
2,3-Butanediol	−0.82	−1.25	NA	NE
cis-CHD	−0.19	0.31	NA	NE
GMB	−0.34	−0.23	NA	NE
Ethyl ether	0.95	1.65	−0.12	−0.18
Tetrahydrofuran	0.46	0.63	NA	NE
Dioxane	−0.45	−0.37	NA	NE
Ethoxyethanol	−0.61	−0.44	−2.42	−2.53
i-Propoxyethanol	−0.04	0.07	−2.11	−2.41

of 1 or 0 depending on whether the atom is an sp^3 carbon to which no heteroatom is attached ($N_C = 1$, others equal 0), an sp^3 carbon to which a heteroatom is attached ($N_{CX} = 1$), an aromatic carbon ($N_{AR} = 1$), or some other atom type (all three equal 0). The $(\epsilon_{curr}\text{-}10)/8$ factor of Eq. 3 varies linearly from 0 to −1.0 going from an ϵ_{curr} of 10 to 2. While there is no formal justification for such a linear relationship, the $\epsilon = 10$ to 2 transition spans only a few angstroms along z, such that a linear relationship should lead to approximately the same results, in practice, as other scaling functions which might be envisioned. The energies predicted by Eq. 3 for virtual polar and nonpolar atoms is represented in the $z = -15$ to $z = -3.1$ region of Fig. 1 *B*.

Eq. 3 stems from the work of El Tayer et al. (1991) who suggested that the differences in water-octanol and water-hydrocarbon partitioning coefficients could be described by a simple relation (Eq. 11 in the former work):

$$\Delta \log P_{\text{HC-octanol}} = 0.12\pi + 1.96\beta + 3.4\alpha + 0.43 \quad (4)$$

where π, α, and β are intrinsic polarizability, hydrogen bond donor, and hydrogen bond acceptor parameters for the *molecule*. From their work and others (Kamlet et al., 1988) *atomic* α and β are readily estimated (since the molecular parameters derive almost exclusively from the presence of heteroatom-containing functionalities) and are reported in Table 1. In deriving Eq. 3 from 4, the 0.12π term was dropped because it is always very small compared to the second two terms (see El Tayer et al. (1991)). A serious problem with Eq. 4 is its failure to take molecular surface area into account (e.g., it would predict nearly identical $\Delta \log P_{\text{HC-oct}}$ for both methanol and decanol). Accordingly, the factor of 0.43 was replaced by a simple function of the number of each of three classes of carbon molecules present in the compound of question: $0.091N_C + 0.31N_{CX} + 0.045N_{AR}$ (see definition of terms as given for Eq. 3). The parameters associated with the three N were calculated by fitting Eq. 3 to the experimental $\Delta G_{HC} - \Delta G_{octanol}$ data listed in Table 2. The uncertainties in the parameters so determined are: 0.091 ± 0.025, 0.31 ± 0.06, and 0.045 ± 0.020.

It should be noted that the current set of P_o, α, and β do not include atomic parameters for atoms with a formal charge, although extension of the set to include such atoms should be straightforward.

Partitioning data

The proposed interfacial energy function was tested for its ability to reproduce water-solvent solute partitioning data

*ΔG_{oct}, water-octanol partitioning energy (negative sign means it favors the aqueous phase).

‡Predicted values from Eq. 2.

§$\Delta G_{HC} - \Delta G_{oct}$, difference between water-hydrocarbon and water-octanol partitioning energies (negative sign means compound favors the octanol phase over the aliphatic hydrocarbon phase).

¶Predicted values from Eq. 3.

‖NA, not available; NE, not estimated. DMB, dimethylbutane; DMA, dimethyl acetamide; GMB, glyceryl monobutyrate; CHD, cyclohexane diol.

according to the following relationship:

$$\Delta G_{\text{part}} = \Sigma G_{H_2O} - \Sigma G_{\text{nonpolar solvent}} \quad (5)$$

where ΣG_{H_2O} and $\Sigma G_{\text{nonpolar}}$ are the summed (over all atoms) interfacial energies calculated from Eqs. 2 and 3 (see below) for the molecule placed in bulk aqueous ($\epsilon = 78.5$, G_{H_2O}) and bulk apolar phase ($\epsilon = 10$ for octanol, $\epsilon = 2$ for hydrocarbon).

Water-solvent partitioning energies were calculating from log K_p data using a 1 M standard state. This is in accord with the units used in the original derivations of P_o, α, and β (Kamlet et al., 1988; El Tayer et al., 1991; Viswanadhan et al., 1989).

The water-octanol and water-hydrocarbon partitioning data utilized in this study (see Table 2) were taken primarily from compilations (Hansch and Leo, 1979; Walter and Gutknecht, 1986; El Tayer et al., 1991). Compounds were selected based on functional group representation and relevance to typical uncharged membrane-associating biomolecules. "Hydrocarbon" refers to partitioning data where the nonpolar phase was hexane, cyclohexane, heptane, or another nonfunctionalized alkane; differences in the properties of these solvents are assumed to be negligible.

Force calculations

Ideally, interfacial forces can be calculated from Eqs. 2 and 3 according to the simple relation:

$$F = -dG_{\text{int}}/dz \quad (6)$$

This force is hereafter referred to as the "standard" force. The z dependency of Eq. 6 is illustrated in Fig. 2 *A* for virtual hydrophobic and virtual polar atoms. As can be observed, the force is not formally continuous because a "dehydrating force" is activated when the atoms pass beyond $z = -3.1$ ($\epsilon_{\text{curr}} = 10$) point in the negative z direction.

In actual molecular dynamics or mechanics calculations employing Eq. 6 problems are sometimes encountered. During energy minimizations, amphiphilic molecules will align properly in the interface only if a starting position is judiciously chosen. In molecular dynamics simulations, a similar practical difficulty is sometimes encountered: lipid-like molecules sometimes leave the interfacial region, never to return within a computationally accessible time scale, despite the fact that, on the average, such molecules should spend much more than 99% of their time at the lipid interface (e.g., *sn*-1, 2-dimyristoylglycerol (Sanders and Schwonek, unpublished results)). Both of the above problems stem from the fact that once an atom has moved into either bulk phase, it experiences no force to push it back toward the interface regardless of how energetically unfavorable it is for it to be in that phase (see Fig. 2 *A*). While this is physically reasonable, the practical difficulties alluded to above are not trivial.

Other investigators appear to have encountered similar difficulties and have dealt with this problem by simply fixing 1 or more atoms of the molecule in cartesian space during calculations (De Loof et al., 1991; Pastor et al., 1991). This

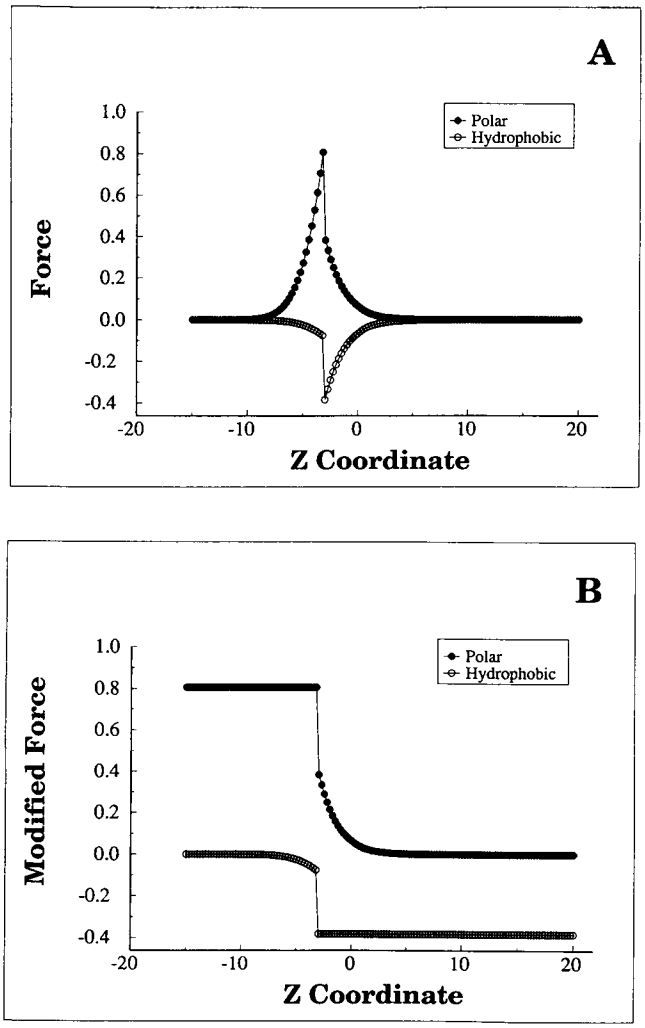

FIGURE 2 Standard (*A*) and "modified" (*B*) forces (kcal mol^{-1} Å^{-1}) as a function of the z coordinate for the virtual polar and nonpolar atoms described in the caption for Fig. 1.

is not a completely satisfactory solution, given that such an anchoring presupposes knowledge of the correct vertical placement of 1 or more atoms in the interface *prior* to calculations and is also unrealistic given that molecules composing liquid crystalline PC bilayers sample a fairly large range of space up and down the bilayer normal (Wiener and White, 1992).

Based on the present work, it is possible to propose a force method which, while falling short of formal justifiability, may be viewed as a significant improvement over fixing some atoms in space. This method leads to what shall be referred to as the "modified" force and can be implemented as follows. At the beginning of a calculation, the maximum possible force exerted on a given atom is calculated. This force will occur either at the point of inflection in the dielectric transition (Eq. 1) or at the $\epsilon > 10$ to $\epsilon < 10$ point (depending upon the P_o, α, β, and N values of the atom in question). For a polar moiety traveling in the negative z (nonpolar) direction, the force is calculated according to Eq. 6 until the z point of maximum force is reached. Once this point

has been passed (on the $-z$ side), the maximum force *continues to be applied* unless the atom moves back in the $+z$ direction past the "maximum force" point (where Eq. 6 takes over again). A converse, but otherwise identical set of force rules can be applied to nonpolar atoms. The "modified force" thus calculated for two virtual atoms is illustrated in Fig. 2 *B*. It should be noted that use of the modified force method is completely inappropriate for some classes of molecules, such as transmembrane polypeptides.

Computational methods

Nonlinear least squares analyses used in the model development described above employed the algorithm of Marquardt and Levinburg as implemented in the program MINSQ (Micromath Software, Salt Lake City, UT).

Molecular modeling (mechanics and dynamics) were carried out on a Silicon Graphics (Mountain City, CA) IRIS 4D-TG33 using routines provided with BIOGRAF (Molecular Simulations, Waltham, MA). The Dreiding II force field (Mayo et al., 1990) was utilized following modification to include the additional interfacial energy/force fields of this paper.

Molecular dynamics (MD) simulations of β-hexyl glucopyranoside (BHEG) within the simulated interface were carried out using the Hoover canonical dynamics algorithm (Hoover, 1985) using a bath temperature of 313 K following a 50-ps equilibration time during which the temperature was ramped from 0 to 313 K. For reasons explained above, the "modified" interfacial force was used in these calculations. Two simulations were carried out. In both cases explicit hydrogens were included only on the sugar headgroup of BHEG. The step size was 2 fs.

The first dynamics calculation (2.4 ns) was intended to lead to the identification of the global minimum structure for interfacial BHEG and thus included "quenching steps" of energy minimization every 2 ps, followed by another cycle of MD.

The second hexyl glucoside simulation (4.8 ns) did not include quenching steps, but included an additional energy/force function designed to simulate lateral surface pressure on the hexyl chain. In spirit, this term is akin to some proposed by Marcelja (1974). An energetic penalty is assigned whenever the alkyl chain is not fully extended along the z axis. If z_1 and z_2 are the z coordinates of the first and last nonhydrogen atoms of the chain and $z_1 - z_2$ is less than its value for an all-*trans* chain aligned along the z axis:

$$E_{\text{chain}} = \textit{weighting factor}/|z_1 - z_2| \qquad (7)$$

If $z_1 - z_2$ is longer than the maximum "aligned all-*trans*" value then E_{chain} is set to 0. From Eq. 7 can be derived a force $(-dE_{\text{chain}}/dz)$. This force is divided by two and applied equally and oppositely to the two terminal carbons of the relevant chain segment. In the case of the second β-hexyl glucoside simulation, the two atoms chosen to define z_1 and z_2 were the terminal methyl carbon of the hexyl chain and the glycosidic oxygen linking the chain to the pyranose ring. The simulation reported in this paper employed a weighting factor of 40 kcal/mol.

Back-calculations of the predicted dipolar and quadrupolar coupling NMR data set from the second dynamics trajectory ensemble file were carried out using the program BANDMODS (Back-Calculation of Anisotropic NMR Data from MOlecular Dynamics Simulations). The primary algorithm of this program is based upon the fact that quadrupolar and dipolar coupling constants are straightforward functions of the time-averaged tensor orientations with respect to the bilayer normal (Sanders and Schwonek, 1992). Dipolar coupling is also a function of the time-averaged internuclear distance between the coupled spins. BANDMODS is available from the authors upon request. A more complete description of this program will be published elsewhere.

RESULTS

Test of Eqs. 2 and 3 for their ability to reproduce water-apolar solvent partitioning data

Given the two-step model for a bilayer interface outlined in the Introduction, a preliminary test of the proposed function would be its ability to reproduce partitioning data for solutes between water and (i), a weakly polar organic phase with hydrogen-bond donating/accepting capabilities or (ii), an effectively anhydrous hydrocarbon phase. Octanol meets the criteria for the first organic phase; it can both donate and accept hydrogen bonds. Furthermore, under conditions of most water-octanol partitioning experiments, octanol is saturated with water such that its concentration is in the range of 2 M (Hansch and Leo, 1979). In the case of water-saturated hydrocarbons, "effectively anhydrous" reflects the fact that water-saturated heptane contains only 5 mM H_2O (Hansch and Leo, 1979).

Water-octanol partitioning

As demonstrated in Table 2, use of the parameters of Table 1, the $2.3 \cdot RT \cdot P_o$ term of Eq. 2, and Eq. 5 led to generally good reproduction of the experimental partitioning data, as expected given that P_o were originally extracted from such data (Viswanadhan et al., 1989). Only in the case of pyridine was the difference between observed and predicted energies greater than 0.7 kcal/mol. It should be noted that the partitioning data set used in this study did not exhaustively test all of the atom types for which parameters are listed in Table 1: focus was made upon molecules containing atom types likely to be encountered in neutral membrane-associating biomolecules.

Water-hexane partitioning

The second term of Eq. 3 was found to be generally successful in replicating the observed differences in partition energies between octanol and hydrocarbon phases (Table 2). Only in the case of glycerol did the deviation between predicted and observed values exceed 0.9 kcal/mol.

Test of the interfacial energy function to reproduce experimental phosphatidylcholine bilayer-water solute partitioning data

A cross-section of water-PC bilayer solute partitioning coefficients were gathered from the literature and converted into the partitioning energies listed in Table 3. Most thermodynamic studies of membrane partitioning utilize the mole fraction or molar standard states (cf. Kamaya et al., 1981; De Young and Dill, 1990).[1] While the parameters used in Eqs. 2–3 were derived from water-solvent partitioning coefficients expressed in molar units, it is unclear that the relevant membrane partitioning data should necessarily be described using this same standard state, considering the fundamental differences between partitioning involving two isotropic phases and partitioning involving an isotropic phase *and* an approximately two-dimensional condensed phase. Accordingly, experimental energies were calculated using both molar *and* mole fraction scales and reported as the ranges spanned by the two values (Table 3).

Equations 1–3, and 6 were integrated into a molecular energy/force field suitable for modeling (see Methods). Most of the molecules of Table 3 were first minimized using only a standard force field with the additional membrane-mimetic terms turned off. Then, ΣG_{int} were measured when the molecules were placed in the bulk aqueous (large $+z$) phase and the hydrocarbon phase (large $-z$) to yield the molecular G_{H_2O} and G_{HC} listed in Table 3. The molecules were then aligned with their long axes in the membrane plane (perpendicular to z) and were subjected to energy minimizations (Dreiding II plus the added membrane terms) which yielded molecular G_{opt}. These calculations were repeated with starting structures in which the long axis of the solute was placed in the xy plane at $z = 0$. It was observed that for each molecule the partitioning energies converged upon nearly identical values from both 0 and 90° oriented starting structures (maximal difference of 0.3 kcal/mol). All minimizations were carried out in duplicate using modified and standard forces with partitioning energies for total energy minimized structures being reported in Table 3. The following paragraphs shall focus solely upon calculations performed using the "standard" force (see Methods). However, as illustrated for most of the molecules in Table 3, the modified force generally leads to similar minimization results.

It can be observed (Table 3) that the predicted partitioning energies ($G_{opt} - G_{H_2O}$) usually fall within the range of "possible" experimental energies (where uncertainty in experimental values stems uncertainty in choice of a standard state). This is particularly encouraging when it is considered that the "observed" ranges listed in Table 3 do not factor in experimental uncertainty.

Benzene and hexane moved through the interfacial region into the low ϵ region. In the case of hexane, this is consistent with experimental neutron diffraction results which locate this molecule at the center of PC bilayers (White et al., 1981). In the case of benzene, while the absolute minimum was observed when benzene is positioned at $\epsilon = 2$, the calculated energy near the interfacial region was observed to be very similar (only 0.2 kcal/mol higher). This lack of a significant preference for either interior or interfacial regions of the bilayer hearkens to experimental observations previously made regarding the distribution of benzene solubilized in nonphospholipid lyotropic liquid crystals (Ward et al., 1986; Boden et al., 1991).

Molecules such as the *n*-alcohols having a polar headgroup and a nonpolar tail and starting with long axes in the xy plane reoriented during minimization such that they align with the z axis.

The glucosides and the peptides presented special problems for the calculations because of the possibility of minimized structures actually representing local minima. The manner is which the glucosides were dealt with is summarized later in the Results section. In the case of the peptides, five to six different starting conformations for each peptide backbone were minimized, with each minimization being run twice: once with the long axis aligned with the z axis at the start of the calculation and once with it aligned in the xy plane (leading to a total of 12–14 minimizations per peptide). For each peptide, at least four of the starting structures converged upon species which exhibited the lowest total energies (within 1 kcal/mol of each other) *and* the lowest partitioning energy (again, all within 1 kcal/mol of each other), suggesting these structures likely lie near the global minimum for both total and partitioning energies for each peptide. Among these sets of final structures, the lowest observed $G_{opt} - G_{H_2O}$ is reported in Table 3. However, within each "minimum" set, both orientational and conformational heterogeneity were observed (structures not shown), suggesting that each peptide can adopt a number of structures all of which lie near the global minimum.

In the case of Ala-Gly-Ala-tBu two families of minima were observed: one with the *t*-butyl group inserted below the $\epsilon = 10$ point of the simulated membrane, with the rest of the molecule lying above this point (in the more polar region); the other structure places the Ala-3 methyl group below $\epsilon = 10$ and the rest of the molecule above this point. Not surprisingly, the latter structures had slightly lower (more unfavorable) partitioning energies at the expense of more favorable total energies compared to the structures in which the *t*-butyl group was "buried."

In the case of the Ala-Phe-Ala-tBu, all of the minima placed the phenyl ring and either the *t*-butyl moiety or the β-methyl of Ala below the $\epsilon = 10$ point, with the rest of the molecule lying in the more polar region of the interface.

Test of the interfacial energy function for reproduction of experimental structural data

Some insight into the potential usefulness of the proposed interfacial energy/force functions of this paper may be pro-

[1] Most recent studies include "volume fraction" values. As far as the author can tell, there is no difference between partition coefficients expressed in molar or in volume fraction units—they are equivalent.

TABLE 3 Predicted and observed partitioning energies (kcal/mol) for various solutes between water and the PC bilayer interface and/or interior

Compound	G_{H_2O}	G_{HC}	G_{opt}	$G_{opt} - G_{H_2O}$ (predicted) (stan. force)	$G_{opt} - G_{H_2O}$ (predicted) (mod. force)	$G_{opt} - G_{H_2O}$ (observed)[a]
Hexane	+2.8	−3.5	−3.4	−6.2	−6.2	−5.9 to −8.1[b]
Benzene	+1.4	−1.5	−1.5	−2.9	−2.9	−2.8 to −5.0[c]
Benzyl alcohol	+0.8	+1.3	−1.5	−2.3	−2.3	−1.2 to −3.4[d]
						−1.6 to −3.8[e]
Ethanol	−0.3	+2.4	−0.6	−0.3	−0.3	+1.6 to −0.6[c]
						+0.4 to −1.8[e]
1-Butanol	+0.6	+1.3	−1.7	−2.2	−2.2	−0.2 to −2.4[c]
						−0.9 to −3.1[f]
1-Hexanol	+1.4	+0.3	−2.7	−4.1	−4.0	−1.9 to −4.1[c]
						−2.3 to −4.5[g]
1-Octanol	+2.2	−0.9	−3.8	−6.1	−6.0	−3.4 to −5.6[g]
β-Hexyl glucoside	0.2	9.8	−4.1	−4.3	−4.3	−1.6 to −3.8[h]
β-Octyl glucoside	1.0	8.8	−5.2	−6.2	−5.9	−2.6 to −4.8[h]
						−5.1 to −7.3[i]
Butyramide	0.5	3.5	−1.7	−2.2	−2.2	+0.3 to −2.0[e]
H_2N-Ala-Phe-Ala-O-*t*-Bu	0.1	9.6	−2.2	−2.3	ND	−2.0 to −4.2[i]
H_2N-Ala-Gly-Ala-O-*t*-Bu	−1.2	+11.0	−1.9	−0.7	ND	−0.7 to −2.9[j]

[a] Values listed here were obtained from literature partition coefficients. Each *range* of values represents the span of energies between the energy calculated using the molar standard state (the first value of the range) and the mole fraction standard state (the second value). According to the convention of this table, a *negative* partitioning energy indicates the solute favors the interface.
[b] DMPC at 45°, De Young and Dill (1990).
[c] DMPC at 30°, De Young and Dill (1988).
[d] Various PC, determined by suppression of T_m, Kamaya et al. (1981).
[e] DMPC at 40°, Katz and Diamond (1974).
[f] Dipalmitoyl PC 50°, Zhang and Rowe (1992).
[g] Egg yolk PC at 25°, Jain and Wray (1978).
[h] Egg yolk PC at 25°, Ram et al. (1992).
[i] Egg yolk PC at 25°, Ueno (1989).
[j] DMPC at 30°, Jacobs and White (1989).

vided by testing the ability of these functions to predict structures for an interfacial biomolecule whose structure has previously been addressed based upon experimental data. For such a test, BHEG was chosen based on the availability of a substantial set of NMR quadrupolar and dipolar coupling data for this compound in liquid crystalline PC bilayers[2] (Sanders and Prestegard, 1991), as well as preliminary interpretations of this data in structural terms (Sanders and Prestegard, 1992; Hare et al., 1993).

Energy minimizations of BHEG were executed starting from conformations in which the pyranose ring was always in the chair conformation, the alkyl chain was always all-*trans*, and the glycosidic linkage was one of five conformations (ϕ,ψ = −120, 180; 60, 180; −120, 90; 0, 180; or −60, 180; see Hare et al. (1993) for convention). Each of these five conformations were minimized from two different starting orientations, one with the long molecular axis along z, one with the axis near $z = 0$ in the xy plane. Eight of these 10 starting structures converged upon three conformations (ϕ, ψ = −150, 180; −75, 73; 53, −177) representing local minima having very similar overall energies (25.4 ± 0.2 kcal/mol) and partitioning energies (−4.1 ± 0.1 kcal/mol). However one of the starting conformers (ϕ,ψ = −60, 180) converged upon a single conformer (ϕ,ψ = −66, −179, from both starting orientations) which exhibited a partitioning energy nearly equivalent to the other six final structures, but which exhibited a lower overall energy (23.3 kcal/mol). While all 10 final structures exhibited similar partitioning energies, they represented a fairly wide range of headgroup orientations with respect to the bilayer normal (not shown).

In order to verify that the global minimum had been reached in the above minimizations, quenched molecular dynamics calculations were also executed (see Methods). From the 1200 minimized (quenched) structures generated during the course of the 2.4-ns dynamics simulation, the 10 lowest energy structures were extracted and examined. These 10 structures exhibited total energies within 0.5 kcal/mol of each other and partitioning energies in the range of −4.3 ± 0.2 kcal/mol. All 10 structures exhibited glycosidic torsion angles very near the lowest energy conformer generated by

[2] The original NMR data set reported was for *β-dodecyl* glucopyranoside. However, subsequent experimental studies (Sanders and Prestegard, 1992) have shown that BHEG gives rise to similar relative magnitudes of ^{13}C-^{13}C and ^{13}C-^{1}H dipolar couplings, indicating that except for whole-body molecular motions the length of the alkyl chain plays little role in defining the head group conformation and dynamics at the interface. We have chosen to perform calculations for the BHEG because it is computationally more efficient, while using the NMR data set for β-dodecyl glucoside because it is larger and of higher quality than that acquired for BHEG.

the minimizations described in the above paragraph (ϕ = −66 ± 3, ψ = 180 ± 10). However, the head group orientations of the 10 minima exhibited considerable diversity (not shown).

Taken together, the minimization/quenched dynamics results suggest that the most favored glycosidic conformation lies near ϕ,ψ = −65, 180, although there appear to be a number of local minima which are close enough in energy to the global minimum to be frequently sampled at room temperature. This conclusion is very similar to that of Hare et al. (1993), based upon their analysis of an experimental NMR data set (Sanders and Prestegard, 1991). Those authors analyzed the data both with and without additional energy modeling and concluded that the experimental data can be satisfied by square well potentials which allow ranges of phi and psi on the orders of −120 to 0° and 130 to 310°, respectively. Furthermore, they proposed that the global energy minimum lies near ϕ = −80, ψ = 180, with a range of structures near this conformation falling within 1 kcal/mol of the minimum. Their modeling also suggested that there is also a local minimum near ϕ,ψ = 60, 180 which lies within 1 kcal/mol of the global minimum, although this last result was not based upon experimental data.

It is significant that the minimization results of this paper suggest that there are a range of head group *orientations* which can be accommodated by structures possessing similar glycosidic conformations and which exhibit similar interfacial energies. This result suggests that the "average headgroup orientation" previously proposed for β-alkyl glucoside at a PC bilayer interface based on order matrix analysis of NMR data is a *virtual* structure in that it reflects the ensemble average, not necessarily the dominant orientation. This issue is explored at greater length in the following section.

Molecular dynamics simulation of β-hexyl glucoside at a simulated phosphatidylcholine interface

A 4.8-ns MD simulation of BHEG was executed using the proposed interfacial energy/force functions of this paper to mimic interfacial polarity/hydrophobicity and a Marcelja-like function to roughly mimic interfacial packing constraints (see Methods). 4.8 ns may not be long enough to fully sample the orientational and conformational space of BHEG, but may be long enough to provide additional insight into the potential usefulness of the proposed energy function.

The results of the MD simulation are depicted in Fig. 3. It can be observed that the glycosidic linkage spends most of its time near a conformation (ϕ = −65, ψ = 180) near the global minimum identified in the previous section. A minor family of conformers having ϕ,Ψ near +60, +180 appears near 4 ns. As noted above, previous work (Hare et al., 1993) also suggested a similar family of conformers to represent a major local minimum for interfacial alkyl glucoside. The internuclear vector between the linking oxygen and the methyl tail of the chain spends >90% of its time within 30° of the bilayer normal. As suggested by the minimization results of the previous section and previous analysis of experimental data (Hare et al., 1993), the head group appears to have access to a wide range of orientations, as illustrated by the time dependence of the C1-C4 and C2-O5 vector orientations. The averaged orientation of the C1-C4 vector is 32°, while that of the approximately orthogonal C2-O5 vector is 72°. These values are in fairly good agreement with the range of possible average values determined by order matrix analysis of the NMR data for interfacial β-alkyl glucoside (27–36° and 74–89° (Sanders and Prestegard, 1992)). Finally, Fig. 3 suggests that the glycosidic carbon significantly populates a range of about 5 Å along the bilayer normal, a range which is similar to that observed to be populated by the ester moieties of L_α-PC (Wiener and White, 1992).

As described above, the MD simulation led to results which were consistent with a number of experimentally derived observations. However, a more stringent test of the validity of the simulation might be its ability to directly reproduce the original NMR data set. This was carried out as described in the Methods and presented in Table 4. As can be observed the MD trajectory file does *not* quantitatively reproduce the NMR dipolar/quadrupolar coupling data set for interfacial β-dodecyl glucoside (Table 4). However, is unclear whether this disagreement stems from basic flaws in the simulation or whether it stems from a problem unrelated to the adequacy of the energy/force field.[3] Given this ambiguity, the successful reproduction of the absolute *signs* of the coupling constants, and the fact that the simulation results are in agreement with a number of experimentally based observations (above paragraph), the molecular dynamics results are relatively encouraging in terms of suggesting practical utility for the proposed interfacial energy function.

DISCUSSION

The model presented in this paper provided a reasonably good reproduction of experimental partitioning and structural data, despite the fact that it is *not* designed to mimic *all* aspects of bilayer-solute interactions. In fact, it is clear that the environment of a lipid bilayer is fundamentally different than a bulk solution (even when variations in polarity are neglected). Lateral surface pressure and the variable order of

[3] One obvious problem may be that a 4.8-ns simulation was not long enough to insure the satisfactory sampling of orientational space. Another potential problem lies in the fact that dipolar and quadrupolar couplings are sometimes hypersensitive to relatively minor variations in internuclear vector orientational ensembles. As a result, it is possible that a simulation could be very nearly correct by most standards and still fail to reproduce the data (as suggested in the case of BHEG by the agreement of the MD-determined averaged headgroup orientation and the corresponding NMR/order matrix determined result). Yet another problem may lie in the fact that the choice of a weighting constant for the "Marcelja-like" energy/force (Eq. 7) was somewhat arbitrarily made. Discernment between the possibilities is a task which will require development of analytical procedures which extend beyond the scope of this paper.

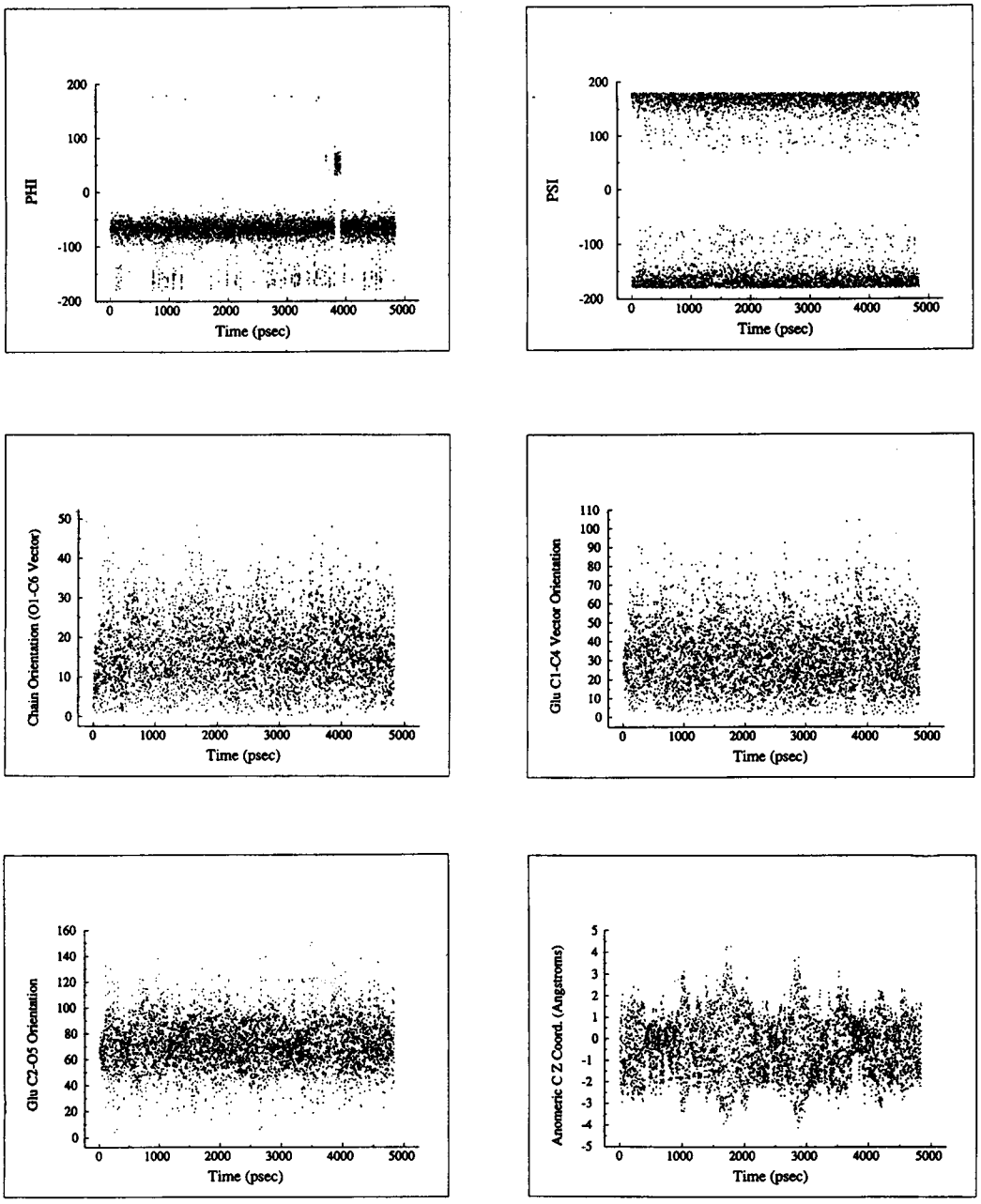

FIGURE 3 Summary of results from the 4.8-ns molecular dynamics simulation of β-hexyl glucoside within the simulated PC interface. All angles are given in degrees. The orientations are with respect to z axis (the bilayer normal).

the molecules composing lyotropic liquid crystalline assemblies place unique constraints upon the modes of insertion and the dynamics of associated solutes (cf., De Young and Dill, 1988, 1990). However, these *unique* constraints are generally *steric* in nature and can be energetically modeled by the use of "Marcelja" functions (Marcelja, 1974; De Loof et al., 1991; Pastor et al., 1991). The model proposed in this paper is designed to describe those aspects of solute-interface interactions which are electrostatic/"hydrophobic" in nature. In a sense, it complements Marcelja-like functions. In the following discussion, the basic approximation of this paper that the hydrophobic/electrostatic component of bilayer-solute interactions can be modeled in terms of molecular interaction with an effectively isotropic medium of varying polarity is examined in light of recent experimental evidence.

Neutron diffraction studies have demonstrated that PC molecules of L_α bilayers oscillate wildly with respect to the *average* plane of the interface (Wiener and White, 1992). For example, the phosphate moiety of PC significantly samples (over a period of time) a range of about 10 Å up and down the bilayer normal, while the distribution of interfacial water is such that it significantly populates areas also frequently sampled by the acyl chains. These results reflect extreme mobility of individual PC molecules: such mobility should tend to entropically diminish the propensity for *specific* solute-PC intermolecular interactions. This conclusion is

TABLE 4 Predicted* and observed‡ dipolar coupling constants for hexyl glucoside at an L_α phosphatidylcholine interface

Relevant atomic pair	Coupling type	Observed	Predicted
		Hz	Hz
Glu C3-D3	quadrupolar	−39800	−81500
Glu C4-D4	quadrupolar	−34600	−83300
Alkyl C1-D1,D1′	quadrupolar	|50400|	−102000
Alkyl C2-D2,D2′	quadrupolar	|46000|	−104000
Glu C1-C2	^{13}C-^{13}C dipolar	−880	−620
Glu C3-C4	^{13}C-^{13}C dipolar	+900	+1340
Glu C4-C5	^{13}C-^{13}C dipolar	−1060	−910
Glu C5-C6	^{13}C-^{13}C dipolar	+880	+1400
Glu C1-C3	^{13}C-^{13}C dipolar	|400|	−602
Glu C1-C4	^{13}C-^{13}C dipolar	|160|	−320
Glu C4-C6	^{13}C-^{13}C dipolar	<|60|	+144
Glu C1-H5	^{13}C-^{1}H dipolar	+5680	+15650
Glu C5-H5	^{13}C-^{1}H dipolar	+5720	+15050

*Predicted couplings from the molecular dynamics simulation of this work. ‡Observed couplings (corrected for an experimental $S_{bilayer}$ of −0.25 accounting for overall bilayer orientation and order) for β-dodecyl glucopyranoside in dimyristoyl phosphatidylcholine bilayers at 40° (Sanders and Prestegard, 1991). See footnote 2.

supported by oriented sample NMR studies (Sanders and Schwonek, 1992; Sanders, 1993) which demonstrated a lack of observable ^{31}P-^{13}C or ^{31}P-^{31}P dipolar coupling between PC and solute molecules or between PC molecules, indicative of intermolecular motions sufficiently dramatic to lead to effectively isotropic averaging of the angles made by the intermolecular phosphorus-carbon vectors with respect to the bilayer normal.

Direct studies of bilayer-solute association also support the notion that solute interactions with individual PC molecules are usually highly nonspecific. For example NMR, surface tension, and calorimetric measurements have failed to discriminate between both bulk and molecular conformational properties of bilayers composed of either L-dipalmitoylphosphatidylcholine (DPPC) or of a 1:1 mixture of L-DPPC and D-DPPC (Arnett and Gold, 1982). Recent oriented sample solid state NMR studies have extended this observation to a much higher level of conformational resolution (Sanders, unpublished results).[4] These results reflect a complete lack of expression of chirality in intermolecular interactions. Oriented sample NMR studies of the weak interfacial association of leucine enkephalin with bilayers have also failed to discriminate between chiral or racemic PC mixtures (Sanders, unpublished results).[5] In another class of studies, the averaged head group orientations of a series of six alkyl glycosides at a PC interface were determined (Sanders and Prestegard, 1992). In all cases, results could be accounted for by approximating the interface as a region of variable polarity in which the pyranose head groups adopt average orientations which maximize polar-polar and hydrophobic-hydrophobic solute-interface interactions. If glycoside-PC interactions were highly specific, it seems improbable that all six test cases would have yielded to such a straightforward interpretation.

Finally, direct measurements of dielectric constants in the interfacial regions of bilayers support the notion of a *gradual* polar to nonpolar transition (Griffith et al., 1974; Brasseur and Ruysschaert, 1986).

The results summarized above support the essential approximation upon which the studies of this paper and previous work (Edholm and Jahnig, 1988; Brasseur et al., 1982; Ram et al., 1992) have been based. This conclusion is further supported by the results of this paper. It is not clear that this approximation can be extrapolated to bilayers containing substantial quantities of lipids besides phosphatidylcholine or to phases other than L_α. Furthermore, while the continuum gradient approximation appears appropriate for use in structural studies, the evidence summarized above does not rule the fact that more specific interfacial electrostatic effects may be present in PC bilayers and can be detected under some circumstances (see Cevc (1990)).

It should be noted that Eqs. 1–3 are designed to deal only with solute-medium interactions, not interface-specific *intramolecular* interactions. Such interactions can readily be treated using Eq. 1 in conjunction with a standard dielectric constant-dependent electrostatic energy function, as described by others (Brasseur et al., 1982).

CONCLUSION

A new method of modeling phosphatidylcholine bilayer interface-solute electrostatic interactions has been presented. The method is very easy to incorporate into existing force/energy fields and should readily be extendable to simulation of an entire bilayer (two interfaces symmetrically juxtaposed) and to the modeling of solute molecules possessing a net charge. While totally empirical, the proposed method reproduces a substantial body of experimental data reasonably well. Undoubtably, functions such as those put forth in this paper will prove most useful when used conservatively and in conjunction with experimental data.

We thank the Herman Frasch Foundation and the taxpayers of the United States for their support of this project (Public Health Service, GM 47485). We also thank Kathleen Howard for a critical reading of an early version of this manuscript.

[4] High resolution oriented sample ^{13}C spectra were acquired from a 50:50 (v/v) D- + L-dimyristoyl PC (DMPC) mixture, in the presence of orientation-promoting L-dihexanoyl PC (DHPC). The spectra are *identical* to those reported in Sanders (1993) and Sanders and Schwonek (1992) for mixtures containing only the L isomer of DMPC.

[5] The ^{13}C spectra have been acquired of leucine enkephalin when mixed with magnetically orientable mixtures of DMPC and DHPC (Sanders and Schwonek, 1992). Association of the peptide with the interface is apparent via the observation of chemical shift anisotropy and ^{1}H-^{13}C dipolar coupling in peptide resonances. The peptide yields an identical spectrum regardless of whether all-L DMPC is used as the primary bilayer component or whether a 50:50 (v/v) D + L mixture is used.

REFERENCES

Arnett, E. M., and J. M. Gold. 1982. Chiral aggregation phenomena. A search for stereospecific interactions between highly purified enantiomeric and racemic DPPC and other chiral surfactants in monolayer,

vesicles and gels. *J. Am. Chem. Soc.* 104:636–639.

Bergethon, P. R., and E. R. Simons. Biophysical Chemistry: Molecules to Membranes. Springer-Verlag, New York, 1990. 340 pp.

Boden, N., S. A. Jones, and F. Sixl. 1991. Use of deuterium NMR as a probe of chain packing in lipid bilayers. *Biochemistry.* 30:2146–2155.

Braiman, M. S., and K. J. Rothschild. 1988. Fourier transform infra-red techniques for probing membrane protein structure. *Annu. Rev. Biophys. Biophys. Chem.* 17:541–570.

Brasseur R., and J.-M. Ruysschaert. 1986. Conformation and mode of organization of amphiphilic membrane components: a conformational analysis. 1986. *Biochem. J.* 238:1–11.

Brasseur, R., M. Deleers, W. J. Malaisse, and J.-M. Ruysschaert. 1982. Conformational analysis of the calcium-A23817 complex at a lipid-water interface. *Proc. Natl. Acad. Sci. USA.* 79:2895–2897.

Cevc, G. 1990. Membrane electrostatics. *Biochim. Biophys. Acta.* 1031: 311–382.

De Loof, H., S. C. Harvey, J. P. Segrest, and R. W. Pastor. 1991. Mean field stochastic boundary molecular dynamics simulation of a phospholipid in a membrane. *Biochemistry.* 30:2099–2113.

De Young, L. R., and K. A. Dill. 1988. Solute partitioning into lipid bilayer membranes. *Biochemistry.* 27:5281–5289.

De Young, L. R., and K. A. Dill. 1990. Partitioning of nonpolar solutes into bilayers and amorphous n-alkanes. *J. Phys. Chem.* 94:801–809.

Edholm, O., and F. Jahnig. 1988. The structure of a membrane-spanning polypeptide studied by molecular dynamics. *Biophys. Chem.* 30:279–292.

El Tayer, N., R.-S. Tsai, B. Testa, P.-A. Carrupt, and A. Leo. 1991. Partitioning of solutes in different solvent systems: the contribution of hydrogen-bonding capacity and polarity. *J. Pharmacol. Sci.* 80:590–598.

Griffith, O. H., P. J. Dehlinger, and S. P. Van. 1974. Shape of the hydrophobic barrier of phospholipid bilayers. *J. Membr. Biol.* 15:159–192.

Hansch, C., and A. Leo. 1979. Substituent Constants for Correlation Analysis in Chemistry, and Biology. J. Wiley and Sons, New York. 339 pp.

Hare., B. J., K. P. Howard, and J. H. Prestegard. 1993. Torsion angle analysis of glycolipid order at membrane surfaces. *Biophys. J.* 64:393–398.

Hoover, W. G. 1985. Canonical dynamics: equilibrium phase-space distributions. *Phys. Rev. A.* 31:1695–1697.

Jacobs, R. E., and S. H. White. 1989. The nature of the hydrophobic binding of small peptides at the bilayer interface: implications for the insertion of transbilayer helices. *Biochemistry.* 28:3421–3437.

Jain, M. K., and L. V. Wray. 1978. Partition coefficients of alkanols in lipid bilayer/water. *Biochem. Pharmacol.* 27:1294–1296.

Kamaya, H., S. Kaneshina, and I. Ueda. 1981. Partition equilibrium of inhalation anesthetics and alcohols between water and membrane of phospholipids with varying acyl chain lengths. *Biochim. Biophys. Acta.* 646: 135–142.

Kamlet, M. J., R. M. Doherty, M. H. Abraham, Y. Marcus, and R. W. Taft. 1988. Linear solvation energy relationships. An improved equation for correlation and prediction of octanol/water partition coefficients of organic nonelectrolytes (including strong hydrogen bond donor solutes). *J. Phys. Chem.* 92:5244–5255.

Katz, Y., and J. M. Diamond. 1974. Thermodynamic constants for nonelectrolyte partition between dimyristoyl lecithin and water. *J. Membr. Biol.* 17:101–120.

Marcelja, S. 1974. Chain ordering in liquid crystals. Structure of bilayer membranes. *Biochim. Biophys. Acta.* 367:165–176.

Mayo, S. L., B. D. Olafson, and W. A. Goddard, III. 1990. Dreiding: a generic force field for molecular simulations. *J. Phys. Chem.* 94:8897–8909.

Milik, M., and J. Skolnick. 1993. Insertion of peptide chains into lipid membranes: an off-lattice Monte Carlo dynamics method. *Proteins Struct. Funct. Genet.* 15:10–25.

Nyholm, P.-B, E. Samuelsson, M. Breimer, and I. Pascher. 1989. Conformational analysis of blood group A-active glycosphingolipids using HSEA calculations. *J. Mol. Recognit.* 2:103–113.

Pastor, R. W., R. M. Venable, and M. Karplus. 1991. Model for the structure of the lipid bilayer. *Proc. Natl. Acad. Sci. USA.* 88:892–896.

Ram, P., E. Kim, D. S. Thomson, K. P. Howard, and J. H. Prestegard. 1992. Computer modeling of glycolipids at membrane interfaces. *Biophys. J.* 63:1530–1535.

Sanders, C. R. 1993. Solid state ^{13}C NMR of unlabeled phosphatidylcholine bilayers: spectral assignments and measurement of carbon-phosphorus dipolar couplings and ^{13}C chemical shift anisotropies. *Biophys. J.* 64: 171–181.

Sanders, C. R., and J. H. Prestegard. 1991. Orientation and dynamics of β-dodecyl glucopyranoside by oriented sample NMR and order matrix analysis. *J. Am. Chem. Soc.* 113:1987–1996.

Sanders, C. R., and J. H. Prestegard. 1992. Headgroup orientations of alkyl glycosides at a bilayer interface. *J. Am. Chem. Soc.* 114:7096–7107.

Sanders, C. R., and J. P. Schwonek. 1992. Characterization of magnetically orientable bilayers in mixtures of DHPC and DMPC by solid state NMR. *Biochemistry.* 31:8898–8905.

Smith, S. O., and O. B. Peersen. 1992. Solid-state NMR approaches for studying membrane protein structure. *Annu. Rev. Biophys. Biomol. Struct.* 21:25–47.

Ueno, M. 1989. Partition behavior of a nonionic detergent, octyl glucoside between membrane and water phases, and its effect on membrane permeability. *Biochemistry.* 28:5631–5634.

Viswanadhan, V. N., A. K. Ghose, G. R. Revankar, and R. K. Robins. 1989. Atomic physicochemical parameters for three dimensional structure directed quantitative structure-activity relationships. Additional parameters for hydrophobic and dispersive interactions and their application for an automated superposition of certain naturally occurring nucleoside antibiotics. *J. Chem. Inf. Comput. Sci.* 29:163–172.

Walter, A., and J. Gutknecht. 1986. Permeability of small nonelectrolytes through lipid bilayer membranes. *J. Membr. Biol.* 90:207–217.

Ward, A. J., S. B. Rananavare, and S. E. Friberg. 1986. Solvation changes induced by a lyotropic lamellar liquid crystal containing solubilized benzene. *Langmuir.* 2:373–375.

White, S. H., G. I. King, and J. E. Cain. 1981. Location of hexane in lipid bilayers determined by neutron diffraction. *Nature (Lond.).* 290:161–163.

Wiener, M. C., and S. H. White. 1992. Structure of a fluid dioleoylphosphatidylcholine bilayer determined by joint refinement of x-ray and neutron diffraction data. *Biophys. J.* 61:434–447.

Zhang, F., and E. S. Rowe. 1992. Titration calorimetric and differential scanning calorimetric studies of the interaction of n-butanol with several phases of dipalmitoylphosphatidylcholine. *Biochemistry.* 31:2005–2011.